JST: Smart Systems and Devices
Volume 34, Issue 1, January 2024, 042-050

Fuzzy Observer-Based Control Design for Rotary Inverted Pendulum Using Takagi-Sugeno Model

Nguyen Thi Van Anh, Dong Bao Trung, Phan Bao Ngoc, Dao Quy Thinh*
Hanoi University of Science and Technology, Ha Noi, Vietnam
**Corresponding author email: thinh.daoquy@hust.edu.vn*

Abstract

The paper introduces fuzzy observer-based control for rotary inverted pendulum systems, renowned for their inherent instability and complexity. We leverage the Takagi-Sugeno (T-S) fuzzy model, which involves the incorporation of local linear models described by fuzzy rules, thus enabling precise and stable control. The Takagi-Sugeno (T-S) fuzzy model, a versatile framework renowned for its suitability in complex control systems, is central to our approach. The significance of observers in accurately estimating unmeasurable states is underlined, with a focus on elucidating the theoretical foundations of fuzzy observers and their role in bolstering control robustness. Additionally, we introduce the integration of Linear Matrix Inequalities (LMIs) and Parallel Distributed Compensation (PDC) for efficient determination of observer and control gains. These advanced tools work in tandem to empower T-S observer control, ensuring both precision and robustness. This paper shows the potential of fuzzy observer-based control and achieving stability and high-performance control of rotary inverted pendulum systems. The effectiveness of the proposed method is validated through simulation results.

Keywords: Takagi-Sugeno fuzzy model, observer control, linear matrix inequality, rotary inverted pendulum.

1. Introduction

The rotary inverted pendulum has captivated the attention of control scientists due to its inherently unstable nature and diverse applications [1-3]. In the pursuit of controlling rotary inverted pendulum systems, researchers have explored various methodologies, including both classical linear control techniques and the advantages offered by nonlinear control. Nonlinear control methods offer a critical advantage in addressing the complex, nonlinear dynamics of the rotary inverted pendulum, where linear approaches often fall short [4].

Among these nonlinear control strategies, fuzzy control, a notable example, plays a pivotal role in managing the intricate and dynamic behavior of the rotary inverted pendulum [5, 6]. Its inherent adaptability and rule-based nature make fuzzy control particularly well-suited for taming the inherent instability of such systems and achieving precise control in control applications. As researching the field of fuzzy control, the Takagi-Sugeno (T-S) fuzzy model emerges as a compelling approach for addressing the complex dynamics [7, 8]. This methodology involves breaking down the system into local linear models, each described by fuzzy rules, which adapt to the varying operating conditions. By combining these local models, the T-S fuzzy control approach offers the capability to provide precise and stable control across a wide range of conditions, making it an appealing choice for tackling the challenges posed by the rotary inverted pendulum.

In the real-world control of systems such as the rotary inverted pendulum, practical constraints often hinder the direct measurement of certain critical states. These limitations stem from factors like sensor inaccuracies or physical restrictions. Consequently, employing an observer becomes not only a necessity but a pragmatic solution to estimate these unmeasurable states accurately. Observers play a crucial role in enhancing the robustness and effectiveness of control strategies in the face of these challenges. We delve into the theory of fuzzy observers and our approach draw inspiration from the well-established Takagi-Sugeno (T-S) model, renowned for its capacity to address complex, nonlinear systems. By constructing a fuzzy observer based on the T-S model, we seek to overcome the challenge of observability and showcase the practical advantages of employing fuzzy observer-based control within the framework of rotary inverted pendulum systems.

In the realm of Takagi-Sugeno (T-S) observer control design, the complexity of the task necessitates the incorporation of advanced tools to derive observer gains and control gains efficiently. Linear Matrix Inequalities (LMIs) and Parallel Distributed Compensation (PDC) stand out as indispensable components of this process. LMIs provide a systematic and effective way to formulate and solve the problems

ISSN: 2734-9373
https://doi.org/10.51316/jst.171.ssad.2024.34.1.6
Received: November 1, 2023; accepted: December 7, 2023

involved in determining observer gains [9, 10]. PDC [11, 12], on the other hand, facilitates the decoupled design of observer and control gains, enhancing the performance of the control system. The synergistic use of these techniques empowers the T-S observer control design to achieve precision and robustness in the challenging context of rotary inverted pendulum systems. This paper, therefore, seeks to contribute to the expanding domain of fuzzy control by providing insights into the application of fuzzy observer-based control and aim to highlight the potential of fuzzy control strategies in achieving stability and high-performance control in the intricate domain of rotary inverted pendulum systems.

2. Fuzzy Observer-Based Control Design

In this section, we delve into the task of modeling the dynamic behavior of the rotary inverted pendulum (RIP). The state equation of the RIP is initially presented, offering a foundation for the subsequent analysis. Following the work in [7], we do the task of transforming the state equation into a Takagi-Sugeno (T-S) fuzzy model. This T-S fuzzy model, characterized by eight premise variables and an 256 fuzzy rules, enables us to capture the nonlinear dynamics of the RIP system.

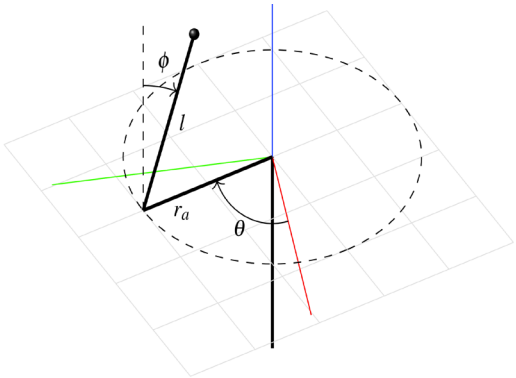

Fig. 1. RIP system

The state equations for the RIP system in Fig. 1 can be expressed as:

$$\ddot{\phi} = 3\begin{pmatrix} d_4 d_5 sin\phi + d_1 d_4 sin^3\phi - d_3 d_5 \dot{\phi} - u_m d_2 d_7 cos\phi \\ +d_2 d_6 \dot{\theta} cos\phi - d_2^2 \dot{\phi}^2 cos\phi sin\phi + 2 d_1 d_2 \dot{\phi}\dot{\theta} cos^2\phi sin\phi \\ +d_1^2 \dot{\theta}^2 cos\phi sin^3\phi + d_1 d_5 \dot{\theta}^2 cos\phi sin\phi - d_1 d_3 \dot{\phi} sin^2\phi \end{pmatrix} \times \left(4 d_1 d_5 - 3 d_2^2 cos^2\phi + 4 d_1^2 sin^2\phi\right)^{-1} \tag{1}$$

$$\ddot{\theta} = -\begin{pmatrix} 4 d_1 d_6 \dot{\theta} - 3 d_2 d_3 \dot{\phi} cos\phi - 4 d_1 d_2 \dot{\phi}^2 sin\phi + 3 d_2 d_4 cos\phi sin\phi \\ +8 d_1^2 \dot{\phi}\dot{\theta} cos\phi sin\phi + 3 d_1 d_2 \dot{\theta}^2 cos^2\phi sin\phi - 4 u_m d_1 d_7 \end{pmatrix} \times \left(4 d_1 d_5 - 3 d_2^2 cos^2\phi + 4 d_1^2 sin^2\phi\right)^{-1} \tag{2}$$

where ϕ, θ are angles of the pendulum and its arm.

The values of d_i, $i = \overline{1,7}$ are calculated using the following formulas:

$$\begin{cases} d_1 = \dfrac{ml^2}{4}, \\ d_2 = \dfrac{mlr_a}{2}, \\ d_3 = B_r, \\ d_4 = \dfrac{mgl}{2}, \\ d_5 = J_{eq} + mr_a^2 + n_g K_g^2 J_m, \\ d_6 = B_a + \dfrac{n_m n_g K_t K_v K_g^2}{R}, \\ d_7 = \dfrac{n_m n_g K_t K_g}{R} \end{cases} \tag{3}$$

where g represents the gravitational acceleration, m signifies the mass of pendulum rod, l denotes the length of pendulum rod, r_a is the length of pendulum arm, J_{eq} corresponds the equivalent moment of inertia considering both the pendulum arm and gears, J_m indicates the moment of inertia of the motor rotor, B_a represents the friction coefficient of the pendulum arm and B_r is the friction of pendulum rod, K_t signifies the torque constant, K_v denotes the motor velocity constant or back EMF constant, R is the motor armature resistance, K_g represents the gearbox ratio, n_g is gearbox efficiency, n_m corresponds motor efficiency and u_m is the control output.

The following T-S fuzzy model can be used to describe the dynamic behaviour of the system:

$$\begin{cases} \dot{x} = Ax + Bu = \sum_{i=1}^{r} h_i(z)\left(A_i x + B_i u\right) \\ y = Cx = \sum_{i=1}^{r} h_i(z) C_i x \end{cases} \tag{4}$$

in which

$$x = \begin{bmatrix} \phi & \theta & \dot{\phi} & \dot{\theta} \end{bmatrix}^T, \; y = \begin{bmatrix} \phi & \theta & \dot{\phi} & \dot{\theta} \end{bmatrix}^T$$

r is number of fuzzy rules,

i corresponds to the i^{th} rule,

h denotes the membership function,

z signifies the premise variable,

A, B are state matrices and A_i, B_i are the sub matrices of fuzzy system.

The membership function $h_i(z)$ has convex sum property like $\sum_{i=1}^{r} h_i(z) = 1, h_i(z) > 0$. The calculation of $h_i(z) = \dfrac{\varpi_i(z)}{\sum_{i=1}^{r} \varpi_i(z)}$ with $\varpi_i(z)$ is grade of each fuzzy rules i , see [7].

Using the equation of state, it is possible to establish a T-S fuzzy model as illustrated below:

$$\begin{cases} A = \begin{bmatrix} 0 & 0 & 1 & 0 \\ 0 & 0 & 0 & 1 \\ a_1 & 0 & a_3 & a_5 \\ a_2 & 0 & a_4 & a_6 \end{bmatrix}, \\ B = \begin{bmatrix} 0 \\ 0 \\ a_7 \\ a_8 \end{bmatrix}, C = \begin{bmatrix} 1 & 0 & 0 & 0 \\ 0 & 1 & 0 & 0 \\ 0 & 0 & 1 & 0 \\ 0 & 0 & 0 & 1 \end{bmatrix} \end{cases} \tag{5}$$

where

$$a_1 = 3\frac{d_4 d_5 sin\phi + d_1 d_4 sin^3\phi}{\phi} \times \left(4d_1 d_5 - 3d_2^2 cos^2\phi + 4d_1^2 sin^2\phi\right)^{-1}$$

$$a_2 = -3\frac{d_2 d_4 cos\phi sin\phi}{\phi} \times \left(4d_1 d_5 - 3d_2^2 cos^2\phi + 4d_1^2 sin^2\phi\right)^{-1}$$

$$a_3 = 3\left(-d_3 d_5 - d_2^2 \dot{\phi} cos\phi sin\phi - d_1 d_3 sin^2\phi\right) \times \left(4d_1 d_5 - 3d_2^2 cos^2\phi + 4d_1^2 sin^2\phi\right)^{-1}$$

$$a_4 = \left(3d_2 d_3 cos\phi + 4d_1 d_2 \dot{\phi} sin\phi\right) \times \left(4d_1 d_5 - 3d_2^2 cos^2\phi + 4d_1^2 sin^2\phi\right)^{-1}$$

$$a_5 = 3\begin{pmatrix} d_2 d_6 cos\phi + d_1^2 \dot{\theta} cos\phi sin^3\phi + d_1 d_5 \dot{\theta} cos\phi sin\phi \\ +2d_1 d_2 \dot{\phi} cos^2\phi sin\phi \end{pmatrix} \times \left(4d_1 d_5 - 3d_2^2 cos^2\phi + 4d_1^2 sin^2\phi\right)^{-1}$$

$$a_6 = -\left(4d_1 d_6 + 3d_1 d_2 \dot{\theta} cos^2\phi sin\phi + 8d_1^2 \dot{\phi} cos\phi sin\phi\right) \times \left(4d_1 d_5 - 3d_2^2 cos^2\phi + 4d_1^2 sin^2\phi\right)^{-1}$$

$$a_7 = \left(-3d_2 d_7 cos\phi\right)\left(4d_1 d_5 - 3d_2^2 cos^2\phi + 4d_1^2 sin^2\phi\right)^{-1}$$

$$a_8 = \left(4d_1 d_7\right)\left(4d_1 d_5 - 3d_2^2 cos^2\phi + 4d_1^2 sin^2\phi\right)^{-1}$$

According to [7], the authors employed the T-S fuzzy model to regulate stability in the RIP system. In this work, the authors elucidated the process of selecting T-S fuzzy rules and ultimately recommended choosing 8 premise variables with 256 fuzzy rules. To formulate the T-S model, choose 8 premise variables following this format:

$$z_1 = \left(4d_1 d_5 - 3d_2^2 cos^2\phi + 4d_1^2 sin^2\phi\right)^{-1}$$

$$z_2 = 3\frac{d_4 d_5 sin\phi + d_1 d_4 sin^3\phi}{\phi}$$

$$z_3 = -3\left(d_3 d_5 + d_2^2 \dot{\phi} cos\phi sin\phi + d_1 d_3 sin^2\phi\right)$$

$$z_4 = -3d_2 d_7 cos\phi,$$

$$z_5 = 3\begin{pmatrix} d_2 d_6 cos\phi + d_1^2 \dot{\theta} cos\phi sin^3\phi + d_1 d_5 \dot{\theta} cos\phi sin\phi \\ +2d_1 d_2 \dot{\phi} cos^2\phi sin\phi \end{pmatrix}$$

$$z_6 = -3\frac{d_2 d_4 cos\phi sin\phi}{\phi}$$

$$z_7 = 3d_2 d_3 cos\phi + 4d_1 d_2 \dot{\phi} sin\phi$$

$$z_8 = -\left(4d_1 d_6 + 3d_1 d_2 \dot{\theta} cos^2\phi sin\phi + 8d_1^2 \dot{\phi} cos\phi sin\phi\right)$$

Consequently, the matrix A and B is updated as follows:

$$A = \begin{bmatrix} 0 & 0 & 1 & 0 \\ 0 & 0 & 0 & 1 \\ z_1 z_2 & 0 & z_1 z_3 & z_1 z_5 \\ z_1 z_6 & 0 & z_1 z_7 & z_1 z_8 \end{bmatrix}, B = \begin{bmatrix} 0 \\ 0 \\ z_1 z_4 \\ 4d_1 d_7 z_1 \end{bmatrix}$$

Hence, the T-S fuzzy model of the RIP system is characterized by 256 fuzzy rules, constructed from 8 premise variables.

3. Control Design

In this section, we embark on the critical phase of control design for the RIP system. Our approach centres on constructing an observer control based on the T-S control model, specially tailored to the complex dynamics of the system. We will also delve into the development of a stability controller. The foundation of our control strategies lies in the adept use of Linear Matrix Inequalities (LMI) and Parallel Distributed Compensation (PDC), allowing us to design control solutions that not only ensure system stability but also offer performance guarantees. Through rigorous proof and analysis, we will demonstrate the effectiveness and reliability of these control methodologies in the intricate domain of RIP systems.

Assumption 1

The variables in the T-S fuzzy model are independent of the estimated state variables. It means that $A_i, B_i, L_i, C_i, h_i(z)$ can be determined without the need for state estimation.

With above assumption, the continuous observer can be expressed as the following:

$$\begin{cases} \dot{\hat{x}} = \sum_{i=1}^{r} h_i(z)\left(\left(A_i \hat{x} + B_i u + L_i(y - \hat{y})\right)\right) \\ \hat{y} = \sum_{i=1}^{r} h_i(z) C_i \hat{x} \end{cases} \tag{6}$$

where *x, y* are the system's state and output vectors and its estimated vector from observer $\hat{x}, \hat{y}$; $h_i(z)$ is the membership function; u is the system input. A_i, B_i, L_i, C_i are the system matrix, control, observation, and output matrices of the system.

Define the estimation error of the observer as:

$$e = x - \hat{x} \tag{7}$$

From equations (4), (6), and (7) we have:

$$\begin{aligned}\dot{e} &= \dot{x} - \dot{\hat{x}} \\ &= \sum_{i=1}^{r} h_i(z)(A_i x + B_i u) \\ &\quad - \sum_{i=1}^{r} h_i(z)\left(A_i \hat{x} + B_i u + L_i(y - \hat{y})\right) \\ &= \sum_{i=1}^{r} h_i(z)(A_i x) \\ &\quad - \sum_{i=1}^{r} h_i(z)\left(A_i(x-e) + L_i\left(\sum_{j=1}^{r} h_j(z) C_j x - \sum_{j=1}^{r} h_j(z) C_j (x-e)\right)\right) \\ &= \sum_{i=1}^{r}\sum_{j=1}^{r} h_i(z) h_j(z)(A_i - L_i C_j)e\end{aligned} \tag{8}$$

The PDC controller is designed based on the state variables from observer as:

$$u = -\sum_{i=1}^{r} h_i(z) F_i \hat{x}. \tag{9}$$

From equations (4), (7), and (9) we have:

$$\begin{aligned}\dot{x} &= \sum_{i=1}^{r} h_i(z)\left(A_i x - B_i \sum_{j=1}^{r} h_j(z) F_j (x-e)\right) \\ &= \sum_{i=1}^{r}\sum_{j=1}^{r} h_i(z) h_j(z)\left((A_i - B_i F_j)x - B_i F_j e\right)\end{aligned} \tag{10}$$

Define $x_\alpha = \begin{bmatrix} x & e \end{bmatrix}^T$, and replace into (8) and (10), we obtain:

$$\dot{x}_\alpha = \begin{bmatrix} \dot{x} \\ \dot{e} \end{bmatrix} = \sum_{i=1}^{r}\sum_{j=1}^{r} h_i(z) h_j(z) \begin{bmatrix} A_i - B_i F_j & B_i F_j \\ 0 & A_i - L_i C_j \end{bmatrix} \begin{bmatrix} x \\ e \end{bmatrix} \tag{11}$$

Let's $G_{ij} = \begin{bmatrix} A_i - B_i F_j & B_i F_j \\ 0 & A_i - L_i C_j \end{bmatrix}$, equation (11) becomes:

$$\begin{aligned}\dot{x}_\alpha &= \sum_{i=1}^{r}\sum_{j=1}^{r} h_i(z) h_j(z) G_{ij} x_\alpha \\ &= \sum_{i=1}^{r} h_i^2(z) G_{ii} x_\alpha + 2\sum_{i=1}^{r}\sum_{i<j}^{r} h_i(z) h_j(z)\left(\frac{G_{ij} + G_{ji}}{2}\right) x_\alpha\end{aligned} \tag{12}$$

Theorem 1

The system described by equation (12) is asymptotically stable if there exists a positive definite matrix *P* that satisfies the following equalities:

$$\begin{cases} G_{ii}^T P + P G_{ii} < 0 \\ \left(\frac{G_{ij} + G_{ji}}{2}\right)^T P + P\left(\frac{G_{ij} + G_{ji}}{2}\right) \le 0 \end{cases} \tag{13}$$

$i < j$ s.t. $h_i(z) \cap h_j(z) \neq \varnothing$.

The roots to Theorem 1 will be obtained through the Lyapunov stability condition. The calculations will be performed using the Yalmip toolbox in Matlab. The Yalmip toolbox in Matlab facilitates the application of the Lyapunov stability condition by providing a user-friendly interface for modeling and solving optimization problems in control theory.

Proof

Considering the Lyapunov function as

$$V(x_\alpha) = x_\alpha^T P x_\alpha \tag{14}$$

From (14) we have

$$\begin{aligned}\dot{V}(x_\alpha) &= \dot{x}_\alpha^T P x_\alpha + x_\alpha^T P \dot{x}_\alpha \\ &= \sum_{i=1}^{r}\sum_{j=1}^{r} h_i(z) h_j(z) x_\alpha^T G_{ij}^T P x_\alpha \\ &\quad + \sum_{i=1}^{r}\sum_{j=1}^{r} h_i(z) h_j(z) x_\alpha^T P G_{ij} x_\alpha \\ &= \sum_{i=1}^{r}\sum_{j=1}^{r} h_i(z) h_j(z) x_\alpha^T (G_{ij}^T P + P G_{ij}) x_\alpha\end{aligned} \tag{15}$$

The system (12) is stable if and only if:

$$G_{ij}^T P + P G_{ij} < 0 \tag{16}$$

Replace (16) into (12)

$$G_{ii}^T P + P G_{ii} + 2\left(\frac{(G_{ij} + G_{ji})^T}{2} P + P\frac{(G_{ij} + G_{ji})}{2}\right) < 0 \tag{17}$$

As a results, we get

$$\begin{cases} G_{ii}^T P + P G_{ii} < 0 \\ 2\left(\frac{(G_{ij} + G_{ji})^T}{2} P + P\frac{(G_{ij} + G_{ji})}{2}\right) \le 0 \end{cases} \tag{18}$$

And the Theorem 1 is concluded.

LMI-based Controller and Observer

Suppose that the Assumption 1 is satisfied and assuming that $B_i F_j e = 0 \; \forall i \le j$, the matrix G_{ij} can be rewritten as

$$G_{ij} = \begin{bmatrix} A_i - B_i F_j & 0 \\ 0 & A_i - L_i C_j \end{bmatrix} \tag{19}$$

Choosing the following positive definite matrix P:

$$P = \begin{bmatrix} P_1 & 0 \\ 0 & P_2 \end{bmatrix} \tag{20}$$

where P_1, P_2 are suitable positive definite matrices. From upper inequality of (13) together with (19) and (20) we obtain:

$$\begin{bmatrix} A_i - B_i F_i & 0 \\ 0 & A_i - L_i C_i \end{bmatrix}^T \begin{bmatrix} P_1 & 0 \\ 0 & P_2 \end{bmatrix} + \begin{bmatrix} P_1 & 0 \\ 0 & P_2 \end{bmatrix} \begin{bmatrix} A_i - B_i F_i & 0 \\ 0 & A_i - L_i C_i \end{bmatrix} < 0 \tag{21}$$

Condition (21) holds true if only:

$$(A_i - B_i F_i)^T P_1 + P_1 (A_i - B_i F_i) < 0 \tag{22}$$

$$(A_i - L_i C_i)^T P_2 + P_2 (A_i - L_i C_i) < 0 \tag{23}$$

Similarly, replace (19), (20) into the lower inequality (13), we obtain the following LMI conditions:

$$(A_i - B_i F_j)^T P_1 + P_1 (A_i - B_i F_j) + (A_j - B_j F_i)^T P_1 + P_1 (A_j - B_j F_i) \le 0 \tag{24}$$

$$(A_i - L_i C_j)^T P_2 + P_2 (A_i - L_i C_j) + (A_j - L_j C_i)^T P_2 + P_2 (A_j - L_j C_i) \le 0 \tag{25}$$

When multiplying both sides of (22) and (24) by $X = P_1^{-1}$ we have:

$$X(A_i - B_i F_i)^T + (A_i - B_i F_i) X < 0 \tag{26}$$

$$X(A_i - B_i F_j)^T + (A_i - B_i F_j) X + X(A_j - B_j F_i)^T + (A_j - B_j F_i) X \le 0 \tag{27}$$

By denoting $M_i = F_i X$ and $N_i = P_2 L_i$, conditions (23), (25), (26), and (27) can be transformed as follows:

$$X A_i^T - M_i^T B_i^T + A_i X - B_i M_i < 0 \tag{28}$$

$$X A_i^T - M_j^T B_i^T + A_i X - B_i M_j + X A_j^T - M_i^T B_j^T + A_j X - B_j M_i \le 0 \tag{29}$$

$$A_i^T P_2 - C_i^T N_i^T + P_2 A_i - N_i C_i < 0 \tag{30}$$

$$A_i^T P_2 - C_j^T N_i^T + P_2 A_i - N_i C_j + A_j^T P_2 - C_i^T N_j^T + P_2 A_j - N_j C_i \le 0 \quad i < j \text{ s.t. } h_i(z) \cap h_j(z) \neq \varnothing \tag{31}$$

Remark

In (31), there exists the condition that: $i < j$ s.t. $h_i(z) \cap h_j(z) \neq \varnothing$. This implies that the condition should be maintained for all $i < j$, excluding the case where $h_i \cap h_j \neq \varnothing$, $h_i(z) \times h_j(z) = \varnothing$ for all z, where $h_i(z)$ denotes the weight of the ith rule. This can be understood as $h_i \cap h_j = \varnothing$ when the i^{th} rule and j^{th} rules do not overlap.

The LMI conditions (28), (29), (30), and (31) can be used instead of the Theorem 1's conditions. The variables X, M_i, P_2, N_i is obtained by using LMI technique. As a results, the controller and observers' parameters are $F_i = M_i X^{-1}$ and $L_i = P_2^{-1} N_i$.

By constructing a common Lyapunov function for all subsystems of the T-S fuzzy system, overall system stability will be achieved when all subsystems, as described by (11), are stable. To attain stability in the subsystems, it is necessary to find a solution that simultaneously satisfies the conditions determined in (28-31). Simultaneously, with the existence of Assumption 1, the separation principle is applied to divide the overall system into two distinct parts, each performing separate tasks: stability control and observation.

4. Simulation Results

The simulation is carried out based on the following initial conditions:

$$\begin{cases} \phi \in \left[-\frac{\pi}{3}; \frac{\pi}{3}\right] (rad) \\ \theta \in [0; 2\pi] (rad) \\ \dot{\phi} \in [-2.5; 0.5] (rad/s) \\ \dot{\theta} \in [-0.5; 5] (rad/s) \end{cases} \tag{32}$$

The parameters for the RIP system are derived from the parameters of the inverted pendulum of Quanser, as outlined in [7].

$$\begin{cases} g = 9.81 \ (m/s^2); \\ l = 0.335 \ (m); \\ m = 0.125 \ (kg); \\ r_a = 0.215 \ (m); \\ J_{eq} = 3.5842 \times 10^{-3} \ (kgm^2); \\ J_m = 3.87 \times 10^{-7} \ (kgm^2); \\ B_a = 0.004 \ (Nms/rad); \\ K_t = 7.67 \times 10^{-3} \ (Nm/A); \\ B_r = 0.0095 \ (Nms/rad); \\ K_v = 7.67 \times 10^{-3} \ (Vs/rad); \\ R = 2.6 \ (\Omega); \\ K_g = 70; \\ n_g = 0.9; \\ n_m = 0.69. \end{cases}$$

The upper and lower boundary of premise variables are obtained and provided in Table 1.

Table 1. The boundary of premise variables.

Premise variables	Boundary values	
	$z_{\min}$	$z_{\max}$
z_1	0.5665×10^{4}	1.0583×10^{4}
z_2	68.0000×10^{-4}	71.0000×10^{-4}
z_3	-4.5624×10^{-4}	-17.0000×10^{-4}
z_4	-2.7447×10^{-4}	-8.6590×10^{-4}
z_5	1.6960×10^{-4}	11.0000×10^{-4}
z_6	-28.0000×10^{-4}	-11.0000×10^{-4}
z_7	-0.726×10^{-4}	2.0343×10^{-4}
z_8	-12.000×10^{-4}	-8.9050×10^{-4}

The positive definite matrices P_1, P_2 are:

$$\begin{cases} P_1 = \begin{bmatrix} 296244.26 & 73.73 & 40056.28 & 1802.78 \\ 73.73 & 0.05 & 9.98 & 0.46 \\ 40056.28 & 9.98 & 5427.31 & 248.47 \\ 1802.78 & 0.46 & 248.47 & 16.34 \end{bmatrix} \\ P_2 = \begin{bmatrix} 1138.62 & 180.21 & -176.01 & -247.25 \\ 180.21 & 506.56 & -4.44 & -19.24 \\ -176.01 & -4.44 & 32.81 & 50.78 \\ -247.25 & -19.24 & 50.78 & 335.03 \end{bmatrix} \times 10^{-8} \end{cases} \tag{33}$$

Finally, there are the selected rules:

1st Rule

$$\begin{cases} A_1 = \begin{bmatrix} 0 & 0 & 1 & 0 \\ 0 & 0 & 0 & 1 \\ 75.287 & 0 & -2.905 & 2.153 \\ -12.139 & 0 & 12.114 & -9.425 \end{bmatrix}; \\ B_1 = \begin{bmatrix} 0 \\ 0 \\ -9.164 \\ 19.039 \end{bmatrix}; \\ L_1 = \begin{bmatrix} 1.746 & -0.541 & 9.649 & -0.185 \\ -0.544 & 0.664 & -2.978 & 0.082 \\ 9.596 & -2.941 & 63.026 & -2.512 \\ -0.197 & 0.085 & -2.601 & 0.995 \end{bmatrix} \times 10^{5}; \\ F_1 = \begin{bmatrix} -2302.21 & -0.57 & -310.42 & -14.39 \end{bmatrix} \end{cases}$$

16th rule

$$A_{16} = \begin{bmatrix} 0 & 0 & 1 & 0 \\ 0 & 0 & 0 & 1 \\ 75.287 & 0 & -2.905 & -0.768 \\ -29.357 & 0 & 1.795 & -12.207 \end{bmatrix}$$

$$B_{16} = \begin{bmatrix} 0 \\ 0 \\ -9.164 \\ 19.039 \end{bmatrix}$$

$$L_{16} = \begin{bmatrix} 1.751 & -0.551 & 9.637 & -0.203 \\ -0.546 & 0.667 & -2.975 & 0.087 \\ 9.630 & -3.005 & 62.951 & -2.626 \\ -0.199 & 0.086 & -2.599 & 0.999 \end{bmatrix} \times 10^{5}$$

$$F_{16} = \begin{bmatrix} -3360.54 & -0.84 & -454.04 & -20.99 \end{bmatrix}$$

64th rule

$$A_{64} = \begin{bmatrix} 0 & 0 & 1 & 0 \\ 0 & 0 & 0 & 1 \\ 75.287 & 0 & -4.829 & -0.768 \\ -29.357 & 0 & 1.795 & -12.207 \end{bmatrix}$$

$$B_{64} = \begin{bmatrix} 0 \\ 0 \\ -18.329 \\ 19.039 \end{bmatrix}$$

$$L_{64} = \begin{bmatrix} 1.754 & -0.552 & 9.642 & -0.204 \\ -0.547 & 0.668 & -2.977 & 0.087 \\ 9.645 & -3.010 & 62.979 & -2.632 \\ -0.199 & 0.087 & -2.601 & 0.995 \end{bmatrix} \times 10^{5}$$

$$F_{64} = \begin{bmatrix} -5362.43 & -1.33 & -725.61 & -33.53 \end{bmatrix}$$

128th rule

$$A_{128} = \begin{bmatrix} 0 & 0 & 1 & 0 \\ 0 & 0 & 0 & 1 \\ 72.187 & 0 & -4.829 & -0.768 \\ -29.357 & 0 & 1.795 & -12.207 \end{bmatrix}$$

$$B_{128} = \begin{bmatrix} 0 \\ 0 \\ -18.329 \\ 19.039 \end{bmatrix}$$

$$L_{128} = \begin{bmatrix} 1.755 & -0.553 & 9.644 & -0.204 \\ -0.544 & 0.668 & -2.977 & 0.087 \\ 9.655 & -3.014 & 62.993 & -2.634 \\ -0.198 & 0.087 & -2.601 & 0.999 \end{bmatrix} \times 10^{5}$$

$$F_{128} = \begin{bmatrix} -3937.38 & -0.98 & -532.47 & -24.68 \end{bmatrix}$$

256th rule

$$A_{256}=\begin{bmatrix}0 & 0 & 1 & 0\\ 0 & 0 & 0 & 1\\ 38.540 & 0 & -2.578 & -0.410\\ -15.673 & 0 & 0.958 & -6.517\end{bmatrix}$$

$$B_{256}=\begin{bmatrix}0\\ 0\\ -9.785\\ -10.165\end{bmatrix}$$

$$L_{256}=\begin{bmatrix}1.766 & -0.552 & 9.647 & -0.208\\ -0.507 & 0.667 & -2.979 & 0.089\\ 9.722 & -3.008 & 63.025 & -2.662\\ -0.202 & 0.087 & -2.603 & 1.002\end{bmatrix}\times 10^5$$

$$F_{256}=\begin{bmatrix}-5664.39 & -1.41 & -766.09 & -35.19\end{bmatrix}$$

$$C=C_1=C_2=\cdots=C_{256}=\begin{bmatrix}1 & 0 & 0 & 0\\ 0 & 1 & 0 & 0\\ 0 & 0 & 1 & 0\\ 0 & 0 & 0 & 1\end{bmatrix}$$

Specify the initial conditions of both the controller and observer as follows:

$$x_c(0)=\left[\frac{\pi}{12},0,0,0\right]^T,\ x_o(0)=\left[\frac{\pi}{8},\frac{\pi}{24},-0.2,-1\right]^T.$$

Simultaneously, it's essential to consider that the actuator's voltage output is constrained within the range of [-24;24] *V*.

Fig. 2 through Fig. 5 depict the outcomes of the observation board. Fig. 2 and Fig 3 illustrate the error of the system and the observed angle, while Fig. 4 and Fig. 5 present the velocity angle error of observer control.

Analysing the figures referenced as Fig. 2, Fig. 3, Fig. 4, and Fig. 5 reveals a rapid convergence of the estimated values to the actual values within a relatively short timeframe. In approximately 0.5 milliseconds, all estimated states closely align with their real counterparts. Furthermore, the error variation is notably small, hovering around only 0.14 rad in the case of Fig. 2. Conversely, in the remaining scenarios, the error graphs steadily converge to zero, exhibiting no fluctuations beyond the initial conditions. This observation underscores the observer's effectiveness as it efficiently drives the error to zero before any alterations in the real states occur, all without incurring transient changes.

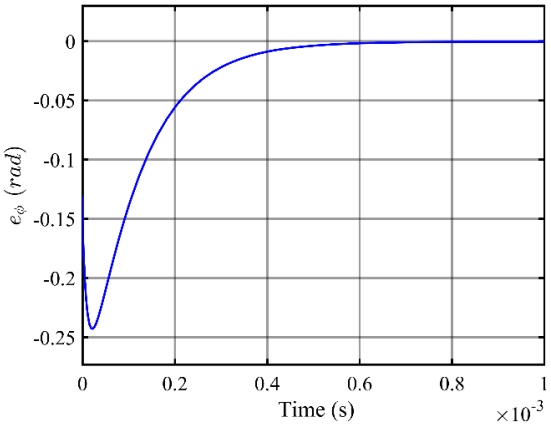

Fig. 2. Error between the system and the observer of angle ϕ.

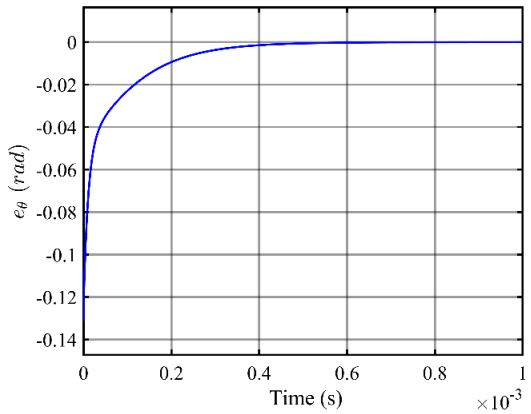

Fig. 3. Error between the system and the observer of angle θ.

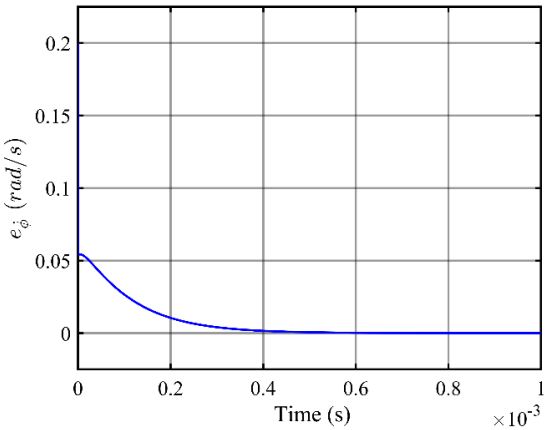

Fig. 4. Error between the system and the observer of angle velocity $\dot{\phi}$.

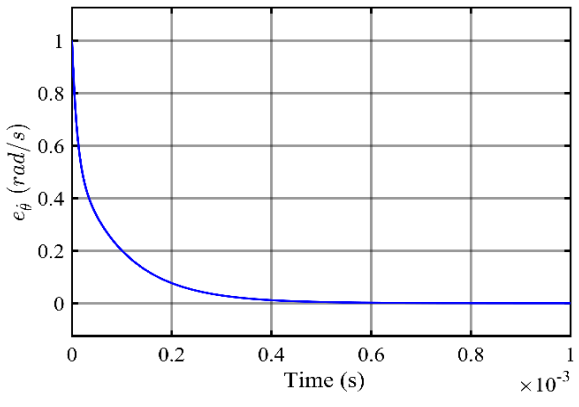

Fig. 5. Error between the system and the observer of angle velocity $\dot{\theta}$.

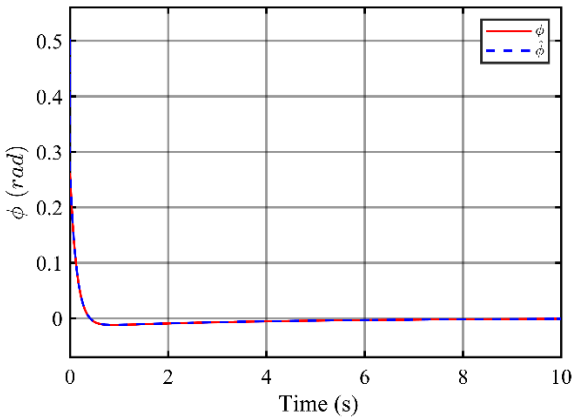

Fig. 6. Angular response ϕ of controller and observer

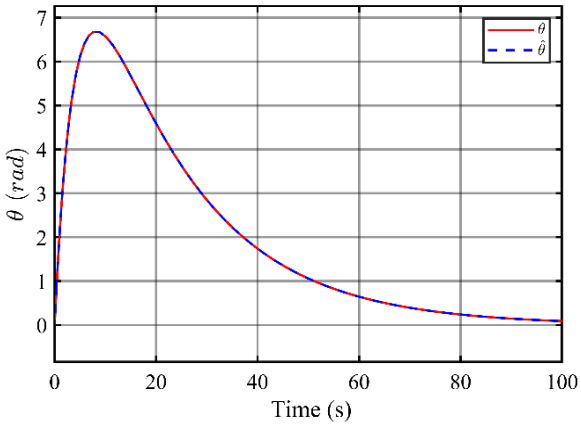

Fig. 7. Angular response θ of controller and observer

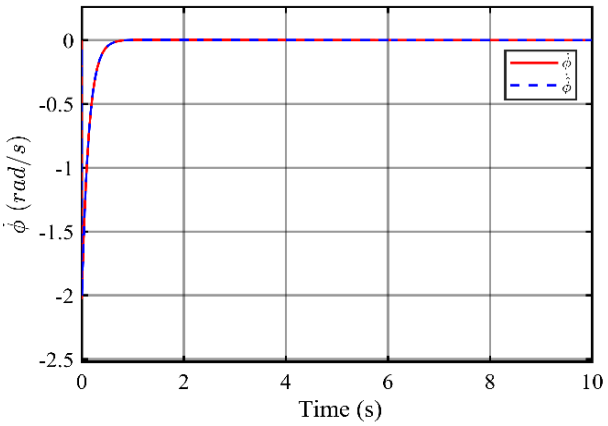

Fig. 8. Angular velocity response $\dot{\phi}$ of controller and observer.

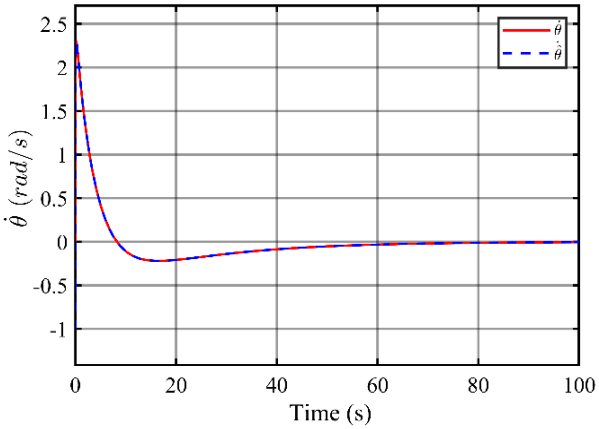

Fig. 9. Angular velocity response $\dot{\theta}$ of controller and observer.

Observing the Fig. 6, Fig. 7, Fig. 8, Fig. 9 underscores the remarkable capability of the observer to faithfully track the controller's trajectory, even in scenarios where the initial conditions of the observer and controller differ. Furthermore, it is evident that the state variables of the actual system attain stability at distinct rates. Variables such as ϕ and $\dot{\phi}$ reach stability within approximately 1s, while $\dot{\theta}$ stabilizes at around 35s and θ requires a substantial 100s to reach true stability.

In stark contrast, the observer swiftly follows the real trajectory in just about 0.5 milliseconds. Moreover, following stabilization, the estimated values remain consistently unaltered when subjected to control signals. This compellingly demonstrates the feasibility of utilizing observers to estimate states or disturbances, even when the initial conditions of these factors are unknown. An intriguing observation is the differing rates at which ϕ and $\dot{\phi}$ attain their steady states in comparison to the relatively gradual return to the original position of θ.

Analysis of the control signal graph in Fig. 10 reveals an initial surge in control voltage to a maximum of 24 V, gradually approaching zero afterward. This behaviour is attributed to the need for voltage to stabilize ϕ once its steady state is reached, thereby restoring θ to its initial position.

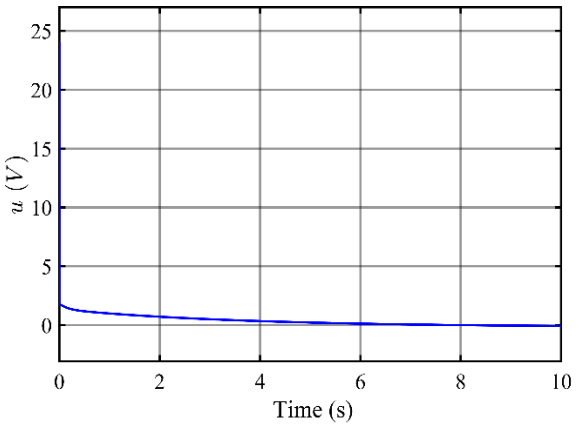

Fig. 10. Control signal.

Due to the modest voltage, the supplied torque remains relatively small, thus explaining the 100 s timeframe required for θ to fully revert. Furthermore, it is noteworthy that even when control signals are restricted to match the actuator's response capacity, both the controller and observer continue to function effectively, underscoring the practical applicability of this approach.

5. Conclusion

This study shows a comprehensive integration of the control and observation of rotary inverted pendulum (RIP) systems, characterized by their inherent instability and complexity. Leveraging the Takagi-Sugeno (T-S) fuzzy model, we have successfully devised control strategies to the management of this systems. Through the integration of observers, we've demonstrated the ability to accurately estimate unmeasurable states. The results have shown the rapid convergence of estimated values to the actual system behavior, highlighting the efficiency of the observer control approach. The combination of LMI and PDC has further fortified the control framework, ensuring stability and control performance. This work contributes to the growing domain of fuzzy control, offering valuable insights into the potential of fuzzy observer-based control for achieving stability and high-performance control in the challenging domain of RIP systems. The results presented here offer promise for further advancements in the field and the development of control solutions for a wide range of complex systems.

Acknowledgments

This research is funded by Hanoi University of Science and Technology (HUST) under project number T2023-PC-036.

References

[1] Pandey, A., & Adhyaru, D. M. Robust control design for rotary inverted pendulum with unmatched uncertainty. International Journal of Dynamics and Control, vol. 11, pp. 1166-1177, Sept. 2022, https://doi.org/10.1007/s40435-022-01047-8

[2] Li, Y., Xin, X., & Yan, Y. A signal compensation-based balance control for the rotary inverted pendulum system. Journal of Vibration and Control, 2023. Online https://doi.org/10.1177/107754632311962

[3] Bhourji, R. S., Mozaffari, S., & Alirezaee, S. Reinforcement learning DDPG–PPO agent-based control system for rotary inverted pendulum. Arabian Journal for Science and Engineering, pp. 1-14, 2023, https://doi.org/10.1007/s13369-023-07934-2

[4] Hamza, M. F., Yap, H. J., Choudhury, I. A., Isa, A. I., Zimit, A. Y., & Kumbasar, T. Current development on using Rotary Inverted Pendulum as a benchmark for testing linear and nonlinear control algorithms. Mechanical Systems and Signal Processing, vol. 116, no. 1, pp. 347-369, 2019, https://doi.org/10.1016/j.ymssp.2018.06.054

[5] Hazem, Z. B., Fotuhi, M. J., & Bingül, Z. Development of a Fuzzy-LQR and Fuzzy-LQG stability control for a double link rotary inverted pendulum. Journal of the Franklin Institute, vol. 357, no. 15, pp. 10529-10556, 2020, https://doi.org/10.1016/j.jfranklin.2020.08.030

[6] AYDIN, M., & Yakut, O., Fuzzy sliding mode control with moving sliding surface of rotary inverted pendulum. Journal of Advanced Research in Natural and Applied Sciences, vol. 8, no. 3, pp. 355-369, 2022, https://doi.org/10.28979/jarnas.1015366

[7] Nguyen, T. V. A., Dong, B. T., & BUI, N. T. Enhancing stability control of inverted pendulum using Takagi–Sugeno fuzzy model with disturbance rejection and input–output constraints. Scientific Reports, vol. 13, no. 14412, 2023, https://doi.org/10.1038/s41598-023-41258-3

[8] Y. J. Kim, Y. G. Lee, S. H. Lee and O. M. Kwon, T-S fuzzy controller design for Rotary Inverted Pendulum with input delay using Wirtinger-based integral inequality, In Proc. 22nd International Conference on Control, Automation and Systems (ICCAS), Jeju, Republic of Korea, pp. 890-895, 2022, https://doi.org/10.23919/ICCAS55662.2022.10003811

[9] V. N. Giap, S. -C. Huang, Q. D. Nguyen and T. -J. Su, Disturbance observer-based linear matrix inequality for the synchronization of Takagi-Sugeno fuzzy chaotic systems, in IEEE Access, vol. 8, pp. 225805-225821, 2020, https://doi.org/10.1109/ACCESS.2020.3045416

[10] Valentino, M. C., Faria, F. A., Oliveira, V. A., & Alberto, L. F. Sufficient conditions in terms of linear matrix inequalities for guaranteed ultimately boundedness of solutions of switched Takagi-Sugeno fuzzy systems using the S-procedure. Information Sciences, vol. 572, pp. 501-521, 2021, https://doi.org/10.1016/j.ins.2021.04.103

[11] Chen, C. W., Modeling and fuzzy PDC control and its application to an oscillatory TLP structure. Mathematical Problems in Engineering, vol. 2010, Article ID 120403, 13 pages, 2010. https://doi.org/10.1155/2010/120403

[12] Rajesh, R., & Kaimal, M. R., T–S fuzzy model with nonlinear consequence and PDC controller for a class of nonlinear control systems. Applied Soft Computing, vol. 7, no. 3, pp. 772-782, June 2007, https://doi.org/10.1016/j.asoc.2006.01.014